Supporting Materials for

Cooperation of Zr(IV)-N and Zr(IV)-O coordinate bonds of Zr(IV)-amide ensures the transparent and tough polyacrylamide hydrogels

Chenglong Dong [a], Mengfan Lu [a], Hailong Fan [b] and Zhaoxia Jin [a,*]

[a] Key Laboratory of Advanced Light Conversion Materials and Biophotonics, Department of Chemistry, Renmin University of China, Beijing 100872, People′s Republic of China.

[b] Institute for Chemical Reaction Design and Discovery (WPI-ICReDD), Hokkaido University, N21W10, Kita-ku, Sapporo 001-0021, Japan

* Corresponding author:

E-mail: jinzx@ruc.edu.cn. (Zhaoxia Jin)

Number of pages: 27

Number of tables: 5

Number of figures: 18

Contents

Table S1. The mechanical properties of Zr-PAAm hydrogels.

zirconium salts	concentration (M)	ε_b (mm/mm)	σ_b (MPa)	E (MPa)	W_e MJ m^{-3}
$Zr(NO_3)_4$	0.2	50.2±2.92	2.65± 0.17	0.15±0.04	75.06±6.65
	0.4	48.84±1.25	3.81± 0.07	0.29±0.08	101.3±4.61
	0.6	27.43±1.35	3.99±0.12	0.65±0.11	55.15±5.19
$ZrCl_4$	0.2	45.39±2.99	2.63±0.07	0.17±0.05	71.93±2.92
	0.4	30.38±0.87	3.29±0.22	0.45±0.03	78.88±7.31
	0.6	25.77±1.37	3.28±0.24	0.75±0.10	46.86±6.29
$Zr(SO_4)_2$	0.2	40.9±0.83	1.43±0.07	0.15±0.05	31.28±5.1
	0.4	31.28±1.75	1.34±0.05	0.19±0.01	20.09±1.7
	0.6	33.95±0.89	1.74±0.19	0.23±0.02	26.06±2.77

Table S2. The change of pH values before and after swelling in water for 3 days at 60 ^{o}C.

zirconium salts	sample name	pH of precursor solutions	pH of water after 3 days' swelling
$Zr(NO_3)_4$	0.2-NO_3	0.87	6.18
	0.4-NO_3	0.65	6.37
	0.6-NO_3	0.49	6.10
$ZrCl_4$	0.2-Cl	0.54	6.40
	0.4-Cl	0.32	6.27
	0.6-Cl	0.15	6.33
$Zr(SO_4)_2$	0.2-SO_4	0.72	6.48
	0.4-SO_4	0.68	6.27
	0.6-SO_4	0.58	6.34

Table S3. The mechanical properties of water-swelled Zr-PAAm(s) hydrogels (3 days, 60 °C).

zirconium salts	concentration (M)	ε_b (mm/mm)	σ_b (MPa)	E (MPa)	W_e MJ m^{-3}
$Zr(NO_3)_4$	0.2	5.43±0.69	0.38±0.04	0.10±0.03	0.91±0.19
	0.4	13.63±1.22	2.45±0.19	0.34±0.01	34.16±4.19
	0.6	7.48±0.38	4.22±0.13	1.34±0.09	20.86±1.43
$ZrCl_4$	0.2	8.55±0.36	0.61±0.07	0.06±0.02	2.66±0.20
	0.4	12.40±1.33	3.65±0.36	0.95±0.02	21.73±4.09
	0.6	6.57±0.64	5.54±0.13	7.98±0.38	29.65±0.92
$Zr(SO_4)_2$	0.2	2.54±0.21	0.13±0.02	0.06±0.02	0.14±0.03
	0.4	12.23±0.04	1.56±0.38	0.25±0.02	14.24±0.05
	0.6	9.42±0.60	3.66±0.08	0.80±0.04	22.55±1.97

Table S4a. The *RGB* value of the different interference colors of dried Zr-PAAm (0.4-NO_3) hydrogels under different tensile strains.

Strain (mm/mm) / *RGB* value	3	6	8	11	14	20	34	47
R	202	231	176	4	27	204	229	188
G	177	158	50	89	151	171	132	94
B	164	26	100	182	136	5	87	155

Table S4b. The *RGB* value of the different interference colors of dried Zr-PAAm (0.4-Cl) hydrogels under different tensile strains.

Strain (mm/mm) / *RGB* value	6	14	23	30	40
R	211	232	222	197	155
G	186	165	111	72	49
B	171	29	18	111	173

Table S4c. The *RGB* values of the different interference colors of dried Zr-PAAm (0.4-SO_4) hydrogels under different tensile strains.

Strain (mm/mm) / *RGB* value	3	14	17	21	25	30	33
R	187	191	141	12	0	80	118
G	163	102	34	61	115	156	167
B	167	2	89	148	145	80	36

Table S5. The *RGB* values of the interference colors of Zr-PAAm (0.4-NO_3) dried gel under different tensile strains.

Strain (mm/mm) / *RGB* value	6	8	11	14	20	34
R	0	75	206	50	195	102
G	26	152	73	205	125	205
B	165	65	156	50	121	170

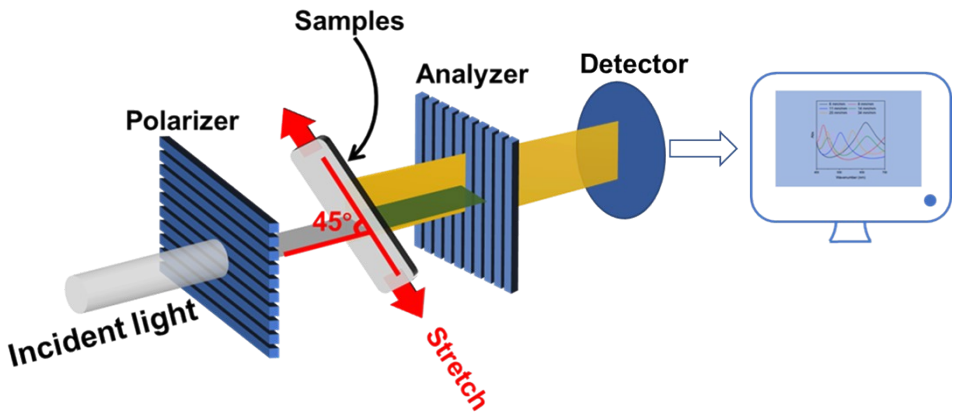

Figure S1. The schematic illustration for the measurement of polarized UV-Vis spectra of stretched samples.

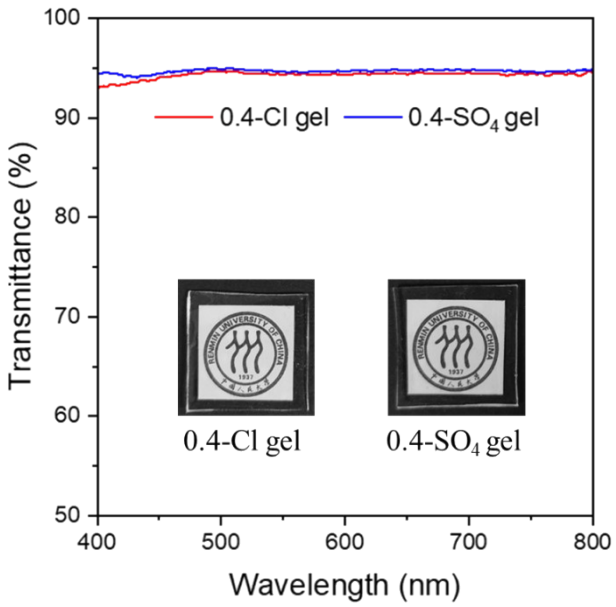

Figure S2. The transmittance of Zr-PAAm (0.4-Cl) and Zr-PAAm (0.4-SO_4) hydrogels. The inset images showed the high transparency of these Zr-PAAm hydrogels. The thickness of hydrogels was about 1.0 mm.

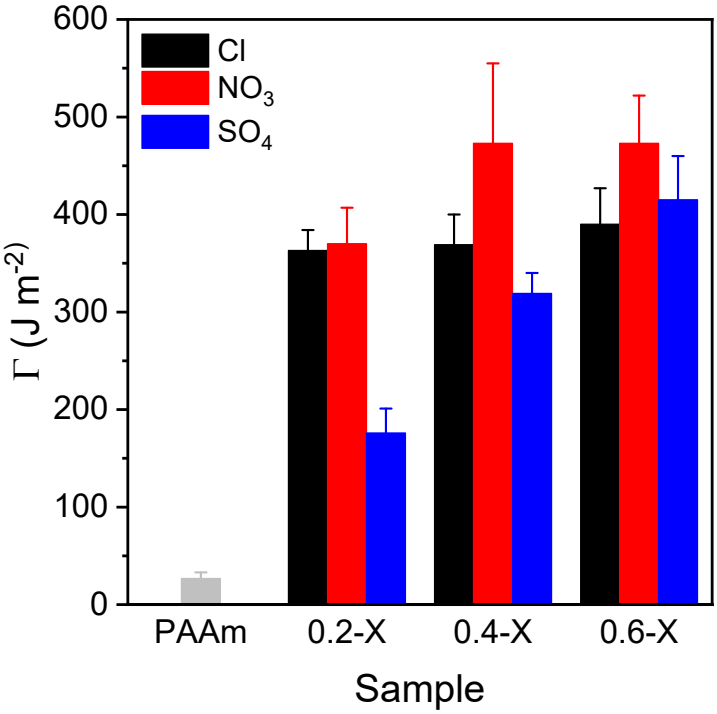

Figure S3. The fracture energy (Γ) of covalently crosslinked PAAm hydrogels and Zr-PAAm hydrogels.

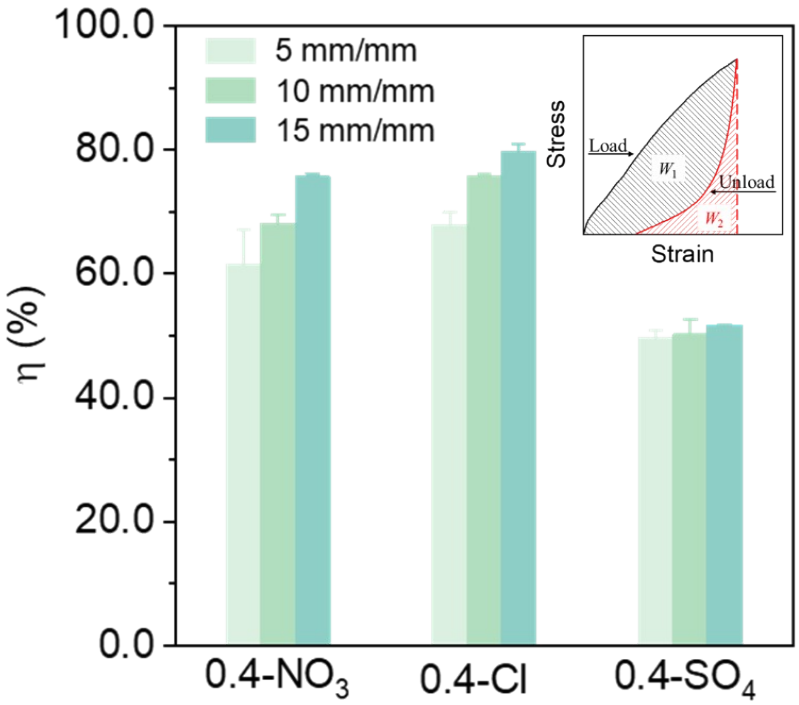

Figure S4. The energy dissipation coefficient of Zr-PAAm hydrogels at various strains (5 mm/mm, 10 mm/mm, 15 mm/mm). The inset showed the integral value of W_1 and W_2.

The energy dissipation coefficient (η) was calculated from the following equation:

$$\eta = \frac{W_1}{W_1 + W_2}$$

Where W_1 was the area under the loading curve (marked by black color) and W_2 was the area under the unloading curve (marked by red color), as shown in the inset.

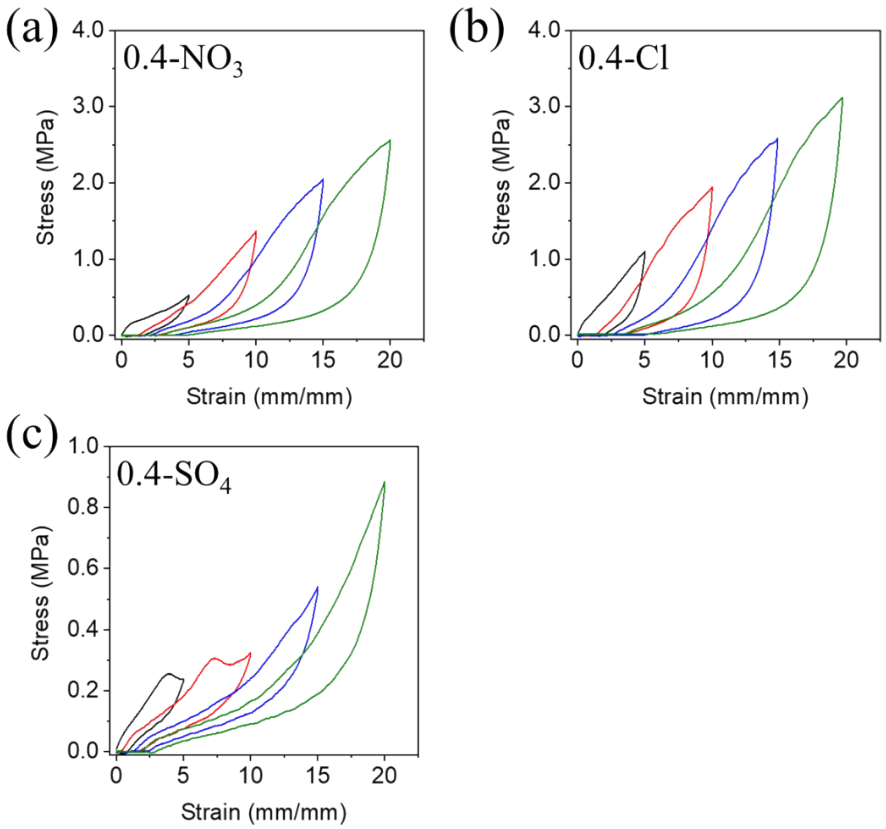

Figure S5. The successively tensile loading-unloading curves of one hydrogel with the increasing strain (ε_m=5 mm/mm, 10 mm/mm, 15 mm/mm, 20 mm/mm).

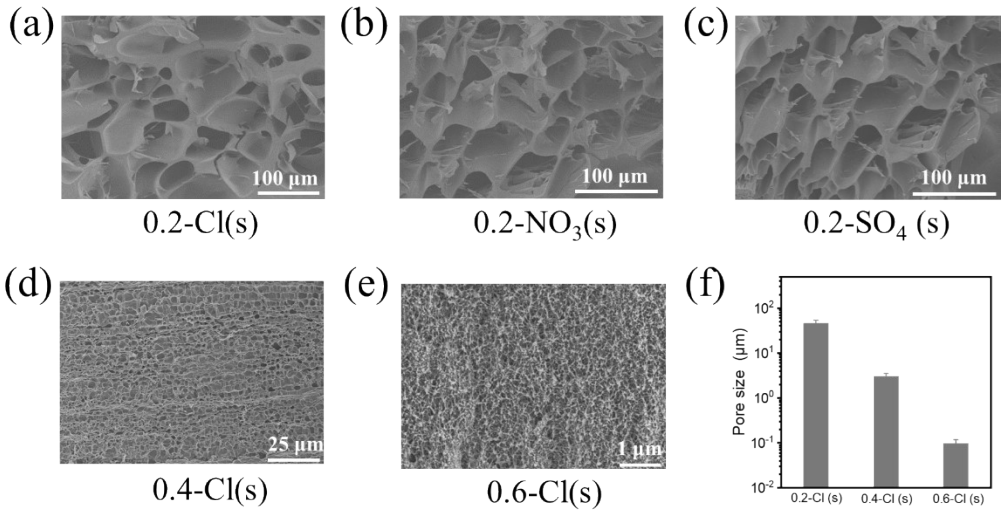

Figure S6. SEM images of Zr-PAAm (0.2-X(s)) hydrogels (a-c), Zr-PAAm (0.4-Cl(s)) (d), Zr-PAAm (0.6-Cl(s)) (e), and the comparison of pore sizes of Zr-PAAm (*m*-Cl(s)) hydrogels (f).

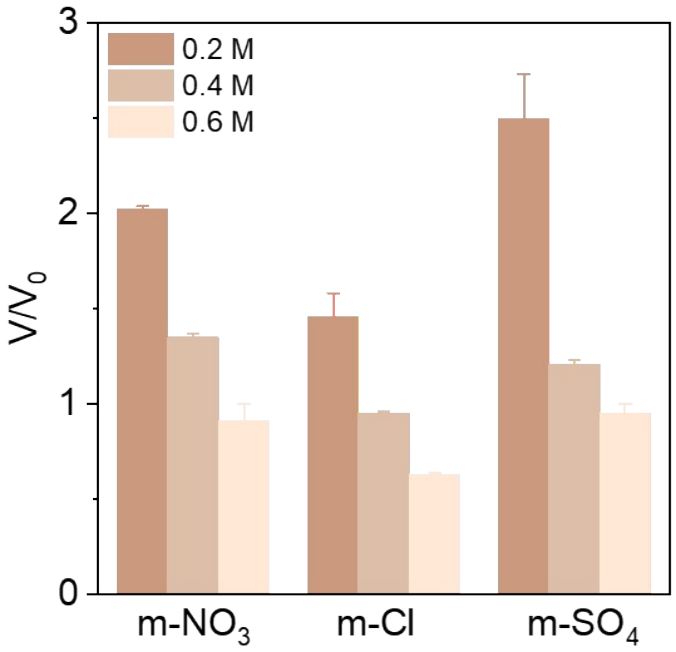

Figure S7. The size variations of Zr-PAAm hydrogels after swelling in water for 3 days at 60 ºC. The V_0 and V represented the volume of as-prepared Zr-PAAm and swollen Zr-PAAm(s) hydrogels, respectively.

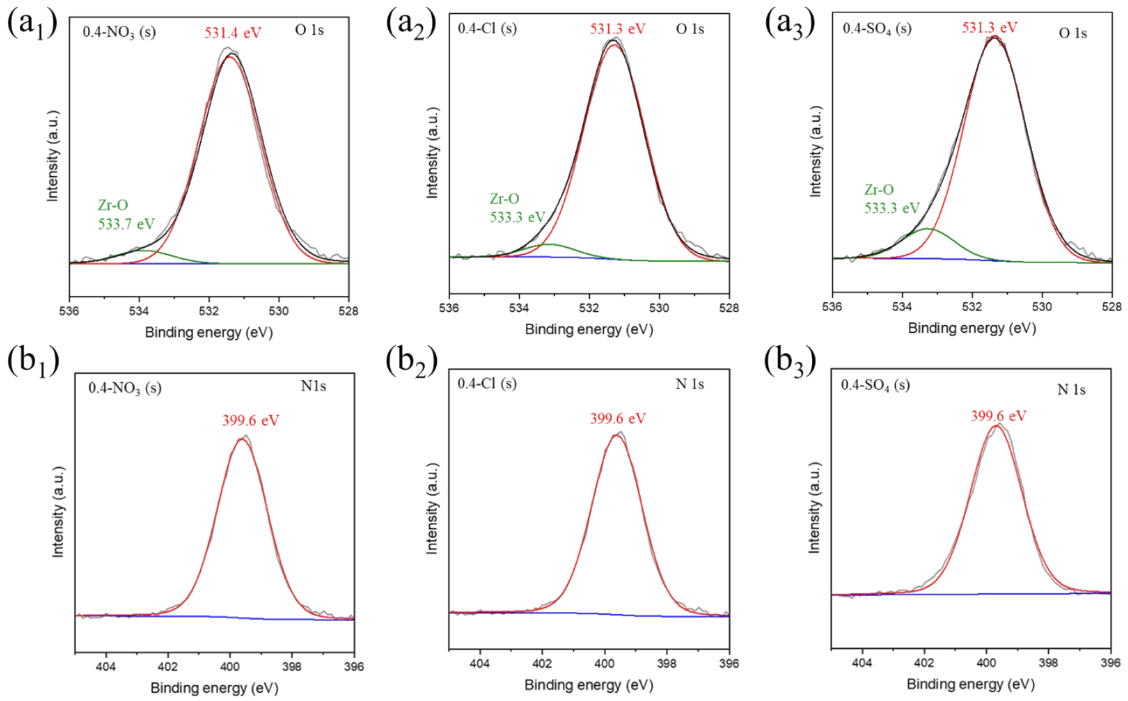

Figure S8. High-resolution XPS spectra of deconvoluted (a) O 1s and (b) N 1s of Zr-PAAm(s) hydrogels.

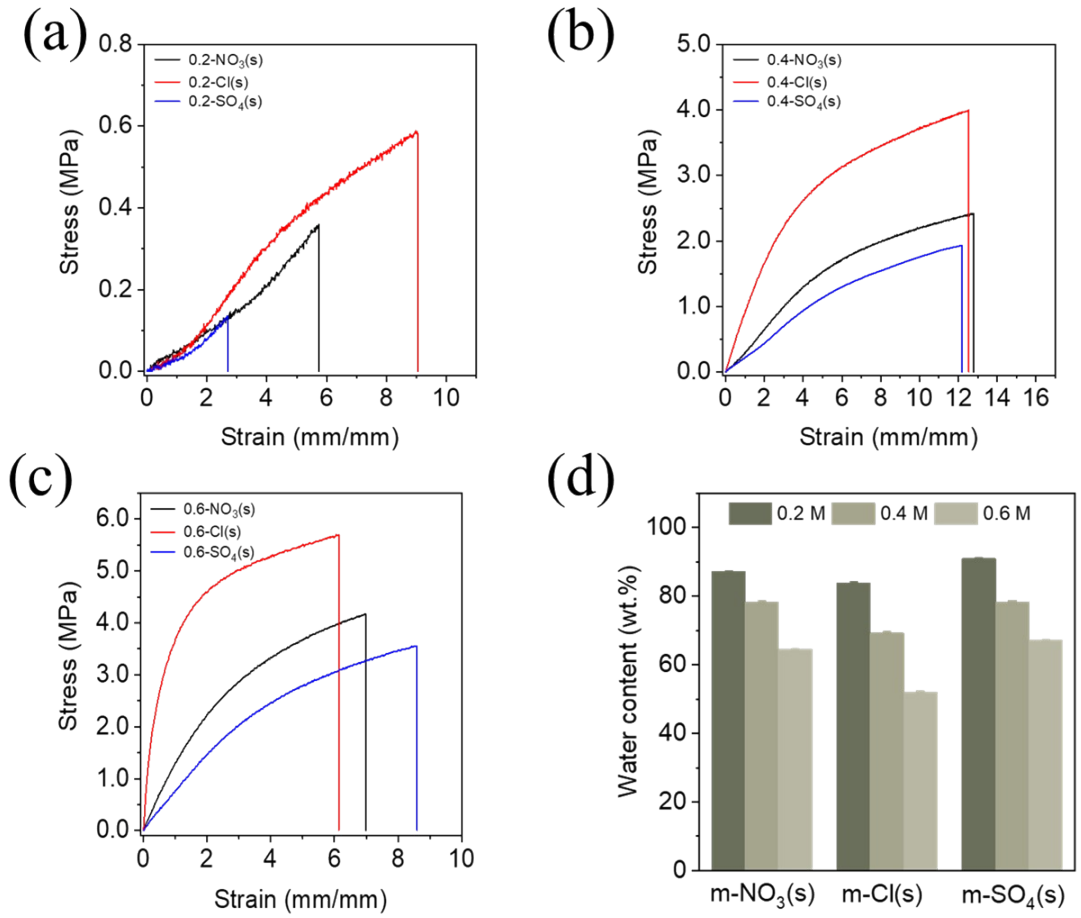

Figure S9. The properties of Zr-PAAm hydrogels after swelling in water for 3 days at 60 ºC. (a-c) The tensile curves. (d) The water content.

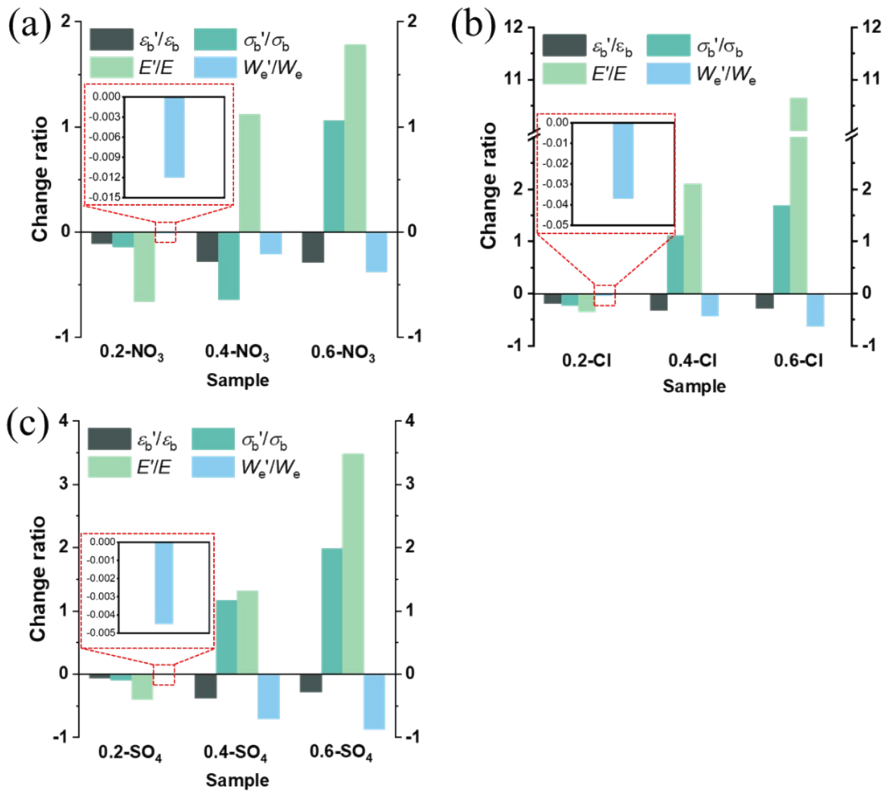

Figure S10. The summary of the change ratios of the fracture strain (ε_b), fracture stress (σ_b), elastic modulus (E), toughness (W_e) of Zr-PAAm hydrogels before and after swelling (with the apostrophe ′) in water for 3 days at 60 ºC. (a) Zr-PAAm (*m*-NO_3) hydrogels, (b) Zr-PAAm (*m*-Cl) hydrogels, (c) Zr-PAAm (*m*-SO_4) hydrogels.

The negative change ratio indicated a decreased property after swelling. For example, as shown in Figure S10a, the W_e'/W_e value of 0.2-NO_3 hydrogel was about -0.012, representing the W_e of 0.2-NO_3(s) hydrogels was 0.012 times as small as that of 0.2-NO_3 hydrogels. The positive change ratio indicated the enhanced properties after swelling. For example, as shown in Figure S10b, the W_e'/W_e of 0.6-Cl hydrogel was about 11, representing the W_e of 0.6-Cl(s) hydrogels was 11 times as high as that of 0.6-Cl hydrogels.

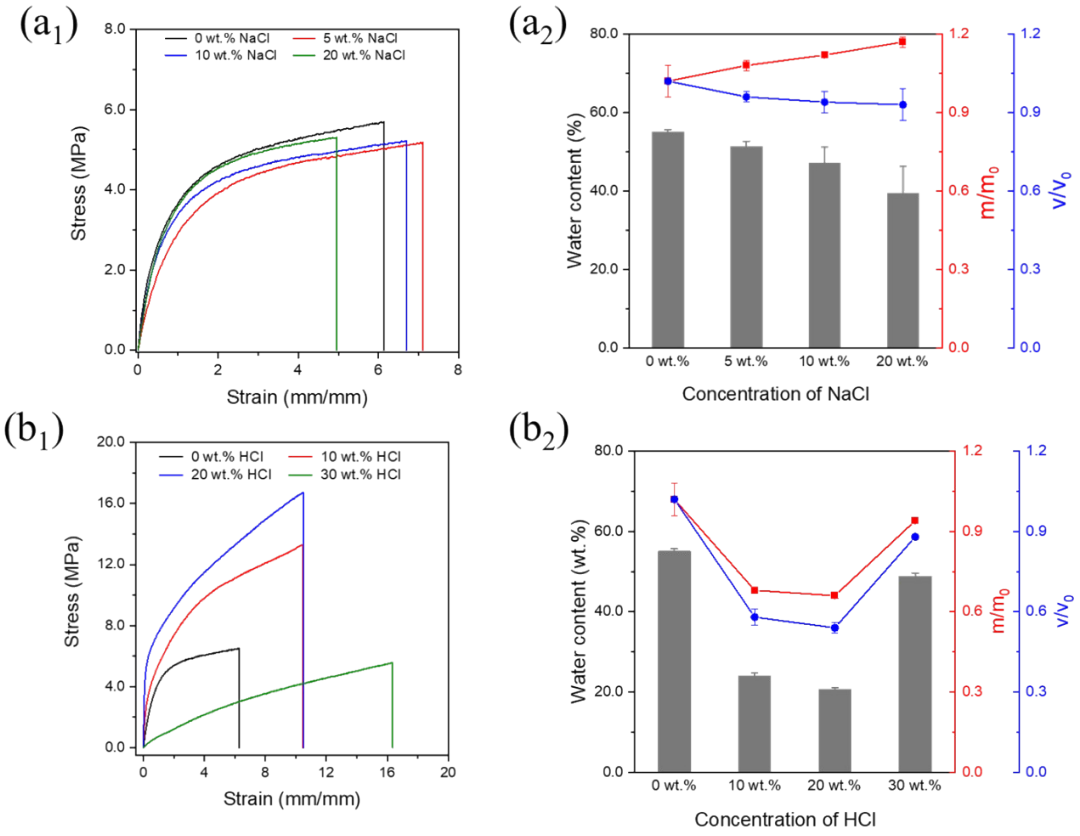

Figure S11. The properties of Zr-PAAm (0.6-Cl(s)) hydrogels after swelling in concentrated (a) NaCl solutions and (b) HCl solution. (a_1, b_1) tensile curves and (a_2, b_2) the water content, the variations of weights and size. The m_0 and v_0 represent the mass and volume of Zr-PAAm (0.6-Cl(s)) hydrogel before swelling, while the m and v are for the mass and volume of Zr-PAAm (0.6-Cl(s)) hydrogel after swelling, respectively.

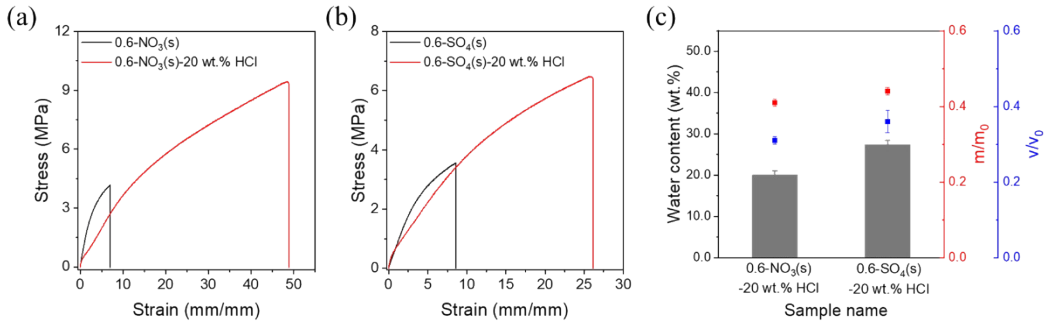

Figure S12. The property changes of Zr-PAAm(s) hydrogels after swelling in 20 wt.% HCl solution for 10 days at room temperature. (a) 0.6-NO_3(s) hydrogels, (b) 0.6-SO_4(s) hydrogels. (c) The water content, the variations of weights, and sizes of 0.6-NO_3(s) and 0.6-SO_4(s) hydrogels. The m/m_0 and v/v_0 represent the change ratios of mass and volume of Zr-PAAm(s) hydrogels after soaking in 20 wt.% HCl solution, respectively.

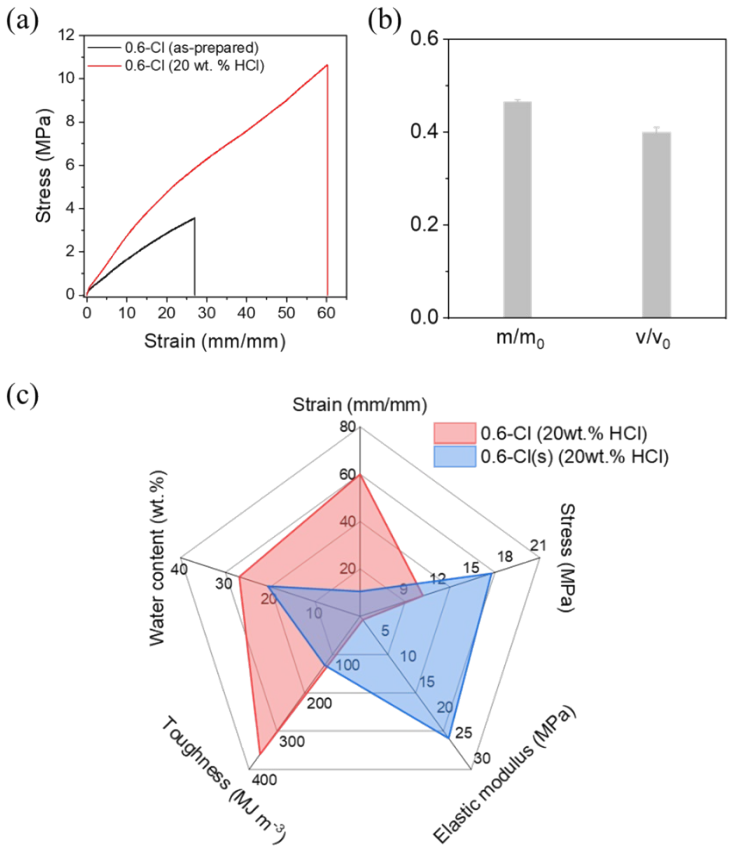

Figure S13. (a) The property changes of as-prepared Zr-PAAm (0.6-Cl) hydrogels after soaking in 20 wt.% HCl solution for 10 days at room temperature. (b) The variations of weights and size of hydrogels after immersion in 20 wt.% HCl solution. The m/m_0 and v/v_0 represent the change ratios of mass and volume of as-prepared 0.6-Cl hydrogels after immersion in 20 wt.% HCl solution, respectively. (c) The comparison of water content, fracture strain, fracture stress, elastic modulus, and toughness of Zr-PAAm (0.6-Cl) and Zr-PAAm (0.6-Cl(s)) hydrogels after immersion in 20 wt.% HCl solution.

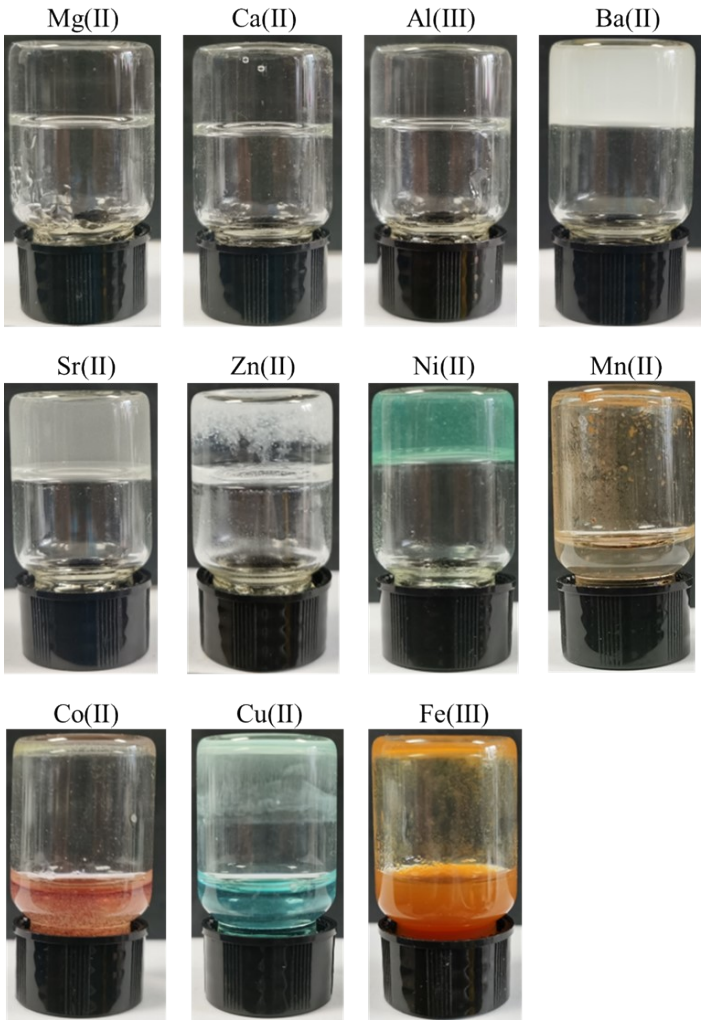

Figure S14. The formation of PAAm hydrogels in the presence of different metal ions. The concentration of different metal ions was kept at 0.2 M. And the preparation process followed that for preparing Zr-PAAm hydrogels.

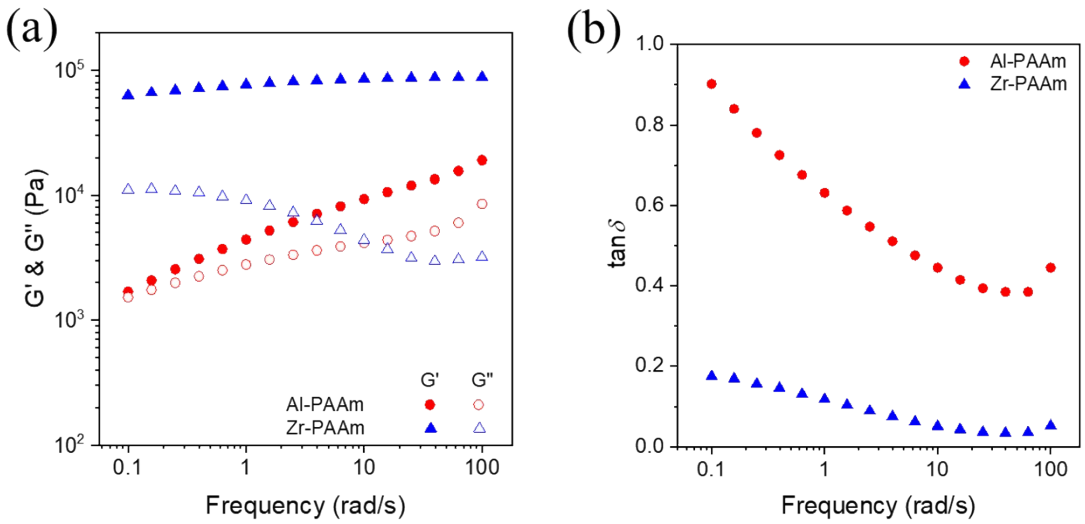

Figure S15. (a) The storage moduli (G′) and loss moduli (G″), (b) loss factor of hydrogels prepared in the presence of $AlCl_3$ or $ZrCl_4$. The concentration of metal ions was kept at 0.2 M.

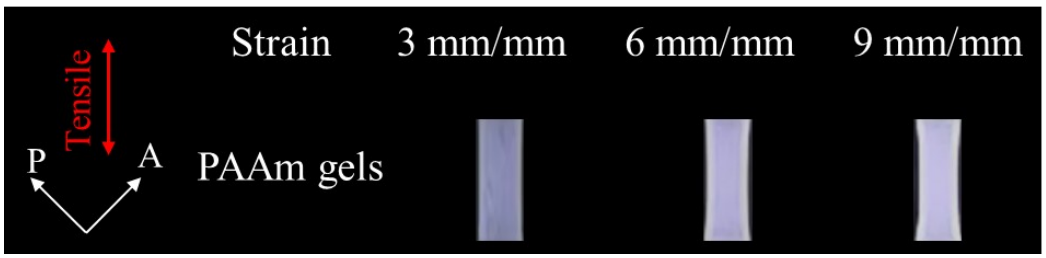

Figure S16. The interference colors of chemically crosslinked PAAm hydrogels under successively increasing tensile strain.

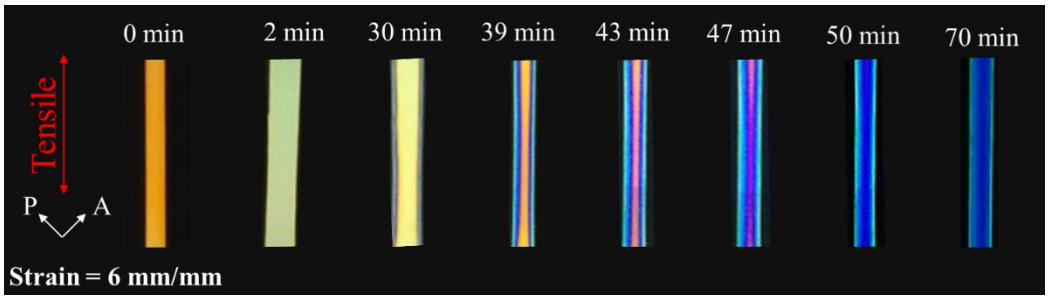

Figure S17. The change of the interference color of a stretched Zr-PAAm (0.4-NO_3) hydrogel kept at 6 mm/mm strain during drying. In the drying process, the orange color of the hydrogel first changed to pale yellow and then to blue, showing the oriented PAAm chains in stretched hydrogel experienced a relaxation at first, then the evaporation of water induced shrinkage of the hydrogels and fixed the orientation of PAAm chains, leading to the increase in the order of interference colors.

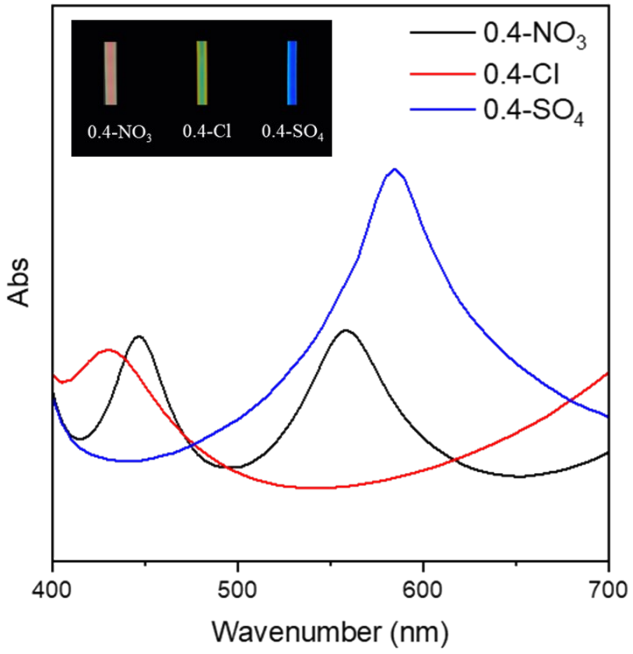

Figure S18. The UV-vis absorption spectra between crossed polarizers of dried 0.4-NO_3, 0.4-Cl, and 0.4-SO_4 gels at 20 mm/mm tensile strains. The inset showed the interference colors of dried gels.

We have calculated the optical path difference (retardation R) based on the UV-vis absorption spectra (Figure S18) and the following equation $S1$[1]:

$$T(R,\lambda) = \sin^2(\frac{\pi R}{\lambda}) \qquad (S1)$$

Where T is the transmittance between crossed polarizers, R is the retardation and λ is the wavelength of incident light.

Reference

1 S. A. Linge Johnsen, J. Bollmann, H. W. Lee and Y. Zhou, *J. Microsc.* 2018, 269, 321-337.